Journal of Solid State Chemistry 183 (2010) 1949–1954

Contents lists available at ScienceDirect

Journal of Solid State Chemistry

journal homepage: www.elsevier.com/locate/jssc

New divalent manganese complex with pyridine carboxylate N-oxide ligand: Synthesis, structure and magnetic properties

Fu-Chen Liu *, Min Xue, Hai-Chao Wang, Jie Ou-Yang *

School of Chemistry and Chemical Engineering, Tianjin University of Technology, Tianjin 300384, PR China

ARTICLE INFO

Article history:
Received 10 February 2010
Received in revised form
15 April 2010
Accepted 20 June 2010
Available online 30 June 2010

Keywords:
Mn(II) complex
Crystal structure
Nicotinate/isonicotinate N-oxide ligands
Topology
Magnetic properties

ABSTRACT

Two new manganese complexes, $[Mn_3(\mathbf{L^1})_4(NO_3)_2]_n$ (**1**, H$\mathbf{L^1}$=nicotinate N-oxide acid) and $[Mn\mathbf{L^2}Cl]_n$ (**2**, H$\mathbf{L^2}$=isonicotinate N-oxide acid)], have been hydrothermally synthesized and characterized by elemental analysis, IR and single-crystal X-ray diffraction. In **1**, the $\mathbf{L^1}$ ligands take two different coordinated modes bridging four and three Mn^{II} ions. The nitrate anions take chelating coordination modes, leading one type of the Mn^{II} ions as a 4-connected node. The whole net can be viewed as a 3, 4, 6-connected 4-nodal net with Schläfli notation $\{4^3\}2\{4^4; 6^2\}4\{4^6; 6^6; 8^3\}$. Complex **2** has a honeycomb layer mixed bridged by chlorine, N-oxide and carboxylate. The adjacent layers are linked by the phenyl ring of $\mathbf{L^2}$ ligand, giving a 3D framework with a $\{3^4; 5^4\}\{3^2;4;5^6;6^6\}$ 4, 6-connect net. Magnetic studies indicate that **1** is an antiferromagnet with low-dimensional characteristic, in which a $-J_1J_1J_2-$ coupled alternating chain is predigested. Fitting the data of **1** gives the best parameters $J_1=-2.77$, $J_2=-0.67$ cm^{-1}. The magnetic properties of complex **2** represent the character of the 2D honeycomb layer with the $J_1=-2.05$ and $J_2=0.55$ cm^{-1}, which results in a whole antiferromagnetic state.

1. Introduction

Coordination polymers draw considerable attention for their fascinating structures and potential applications as functional materials [1,2]. Complexes with attractive topologies and particular properties such as magnetic, optical and adsorbing properties are reported continuously [3,4]. The formation of these complexes depends mainly on the combinations of two factors: the coordination geometry of metal ions and the nature of ligands [5]. Recently, a great variety of new metal organic coordination architectures using flexible ligands has been investigated [6]. The structure of these complexes enriched for the ligands can present different conformations in solid state [7]. The pyridyl N-oxide ligands do not have the swing part like the flexible one but the N-oxide group can bend to metal ions, which makes the coordinated character neither like the rigid one nor the like the flexible one [8]. Among the substituted N-oxide ligands pyridyl-carboxylate are diversity ligands for the carboxylate and N-oxide groups as both can coordinate to metal in different modes [9]. Despite that several complexes containing such ligands were reported; however the oxygen atoms of N-oxide group taking μ_2 mode were seldom in those complexes, and the coordinated chemistry of the ligands needs be comprehended more profoundly [10]. In addition, the investigation of the magnetic interactions conducted by the N-oxide group in such complexes is interesting, especially in the magneto-structural correlations [11].

In this study, two Mn^{II} complex, $[Mn_3(\mathbf{L^1})_4(NO_3)_2]_n$ (**1**, H$\mathbf{L^1}$=nicotinate N-oxide acid) and $[Mn\mathbf{L^2}Cl]_n$ (**2**, H$\mathbf{L^2}$=isonicotinate N-oxide acid)], were synthesized and structurally characterized. Complex **1** is a 2D layer with 3, 4, 6-connected 4-nodal topology, and complex **2** is a 3D structure constructed by honeycomb layers linked by the pyridine ring of $\mathbf{L^2}$. Moreover, magnetic properties of **1** and **2** have been investigated by variable-temperature magnetic susceptibility and magnetization measurements, both of which indicated dominating antiferromagnetic coupling in **1** and **2**. The antiferromagnetic phase transition temperatures are 6.3 K for **1** and 6.2 K for **2**.

2. Experimental section

2.1. Materials and general methods

All the reagents for synthesis were obtained commercially and used as received. Elemental analyses of C, H and N were performed on a Perkin-Elmer 240C analyzer. The FT-IR spectra were recorded from KBr pellets in the range 4000–400 cm^{-1} on a TENSOR 27 (Bruker) spectrometer. The X-ray powder diffraction (XRPD) was recorded on a Rigaku D/Max-2500 diffractometer at

* Corresponding authors.
E-mail addresses: fuchenliutj@yahoo.com (F.-C. Liu), ouyang@tjut.edu.cn (J. Ou-Yang).

0022-4596/$ - see front matter Crown Copyright © 2010 Published by Elsevier Inc. All rights reserved.
doi:10.1016/j.jssc.2010.06.010

40 kV, 100 mA for a Cu-target tube and a graphite monochromator. Simulation of the XRPD spectra was carried out by the single-crystal data and diffraction-crystal module of the Mercury (Hg) program available free of charge via the Internet at http://www.iucr.org. Magnetic data were collected using crushed crystals of the sample on a Quantum Design MPMS XL-7 SQUID magnetometer.

2.2. Synthesis of complexes

$[Mn_3(\mathbf{L^1})_4(NO_3)_2]_n$ (**1**). A solution of $Mn(NO_3)_2$ (1 mmol) (5 ml) was added to methanol solution of H$\mathbf{L^1}$ (0.5 mmol) (10 ml). The mixed solution was sealed in a Teflon-lined stainless-steel vessel, heated at 140 °C for 2 days under autogenous pressure, and then cooled to room temperature. Yellow crystals of **1** were harvested with a yield of ca. 20% based on H$\mathbf{L^1}$. Anal. Calcd. for $C_{24}H_{16}Mn_3N_6O_{18}$: C, 34.27; H, 1.91; N, 9.99%; Anal. Found: C, 34.10; H, 1.87; N, 10.24%. IR (KBr pellet, cm^{-1}): 3445w, 1625w, 1559s, 1398w, 1226s, 1129s, 1023s, 947s, 769s, 576s, 458s.

$[Mn\mathbf{L^2}Cl]_n$ (**2**). A similar process as that of **1** but using $MnCl_2$ (1 mmol) and H$\mathbf{L^2}$ (0.5 mmol) instead, yellow crystals of **2** were obtained with a yield of ca. 20% based on H$\mathbf{L^2}$. FT-IR (KBr pellet, cm^{-1}): 3096, 1360, 1559, 1479, 1399, 1222, 1172, 1147, 885, 887, 786, 388, 660, 641, 449. Anal. Calcd. for $C_6H_4ClMnNO_3$: C, 31.54; H, 1.76; N, 6.13. Found: C, 31.20; H, 1.92; N, 6.40.

2.3. X-ray data collection and structure determinations

Single-crystal X-ray diffraction measurements for **1** and **2** were carried out on a Bruker Smart 1000 CCD diffractometer equipped with a graphite crystal monochromator situated in the incident beam. The determinations of unit cell parameters and data collections were performed with Mo-$K\alpha$ radiation (λ=0.71073 Å) at 294(2) K and unit cell dimensions were obtained with least-squares refinements. The program SAINT [12] was used for integration of the diffraction profiles. All the structures were solved by direct methods using the SHELXS program of the SHELXTL package and refined by full-matrix least-squares methods with SHELXL (semi-empirical absorption corrections were applied using SADABS program) [13]. Metal atoms in each complex were located from the *E*-maps and other non-hydrogen atoms were located in successive difference Fourier syntheses and refined with anisotropic thermal parameters on F^2. The hydrogen atoms of the ligands were generated theoretically onto the specific atoms and refined isotropically with fixed thermal factors. Crystallographic data (excluding structure factors) for **1** and **2** have also been deposited on the Cambridge Crystallographic Data Centre as supplementary publication (nos. CCDC-746388 and 763964). Copies of the data can be obtained free of charge on application to CCDC, 12 Union Road, Cambridge CB21EZ, UK (Fax: (+44) 1223-336-033; e-mail: deposit@ccdc.cam.ac.uk). Details of the X-ray crystal structure analysis of **1** and **2** are summarized in Table 1.

Table 1
Crystal data and structure refinement parameters for complexes **1** and **2**.

	1	2
Chemical formula	$C_{24}H_{16}Mn_3N_6O_{18}$	$C_6H_4ClMnNO_3$
Formula weight	841.25	228.49
Space group	*P*−1	*Pbca*
a (Å)	7.9322(16)	12.987(3)
b (Å)	8.9899(18)	6.5214(13)
c (Å)	10.539(2)	16.539(3)
α (deg)	95.22(3)	90
β (deg)	104.31(3)	90
γ (deg)	98.12(3)	90
V (Å^3)	714.7(2)	1400.8(5)
Z	1	8
D/g (cm^{-3})	1.955	2.167
μ (mm^{-1})	1.406	2.220
T (K)	293(2)	293(2)
R^a/wR^b	0.0689/0.1269	0.0654/0.0857

[a] $R=\Sigma||F_0|-|F_1||/\Sigma|F_0|$.
[b] $R_w=[\Sigma[w(F_0^2-F_c^2)^2]/\Sigma w(F_0^2)^2]^{1/2}$.

3. Results and discussion

3.1. Structure descriptions of complexes *1* and *2*

$[Mn_3(\mathbf{L^1})_4(NO_3)_2]_n$ (**1**). X-ray diffraction analysis reveals that **1** is a 2D coordination network crystallizing in the space group $P\bar{1}$. The asymmetric unit contains one and half Mn^{II} ion, two nicotinate N-oxide anions ($\mathbf{L^1}$), and one nitrate anion (Fig. 1a). Mn1 is located in the inverse center coordinated by six oxygen atoms from six nicotinate N-oxide ligands with Mn–O=2.1–2.3 Å (Fig. 2). Mn2 is coordinated by six oxygen atoms from one nitrate anion in chelating mode and four nicotinate N-oxide ligands with Mn–O=2.0–2.3 Å. In complex **1** there are two types of $\mathbf{L^1}$ ligand. One type of the $\mathbf{L^1}$ bridges Mn1, Mn1E and Mn2 uses the *syn,syn* carboxylate and the oxygen atoms of the N-oxide. The other type of the $\mathbf{L^1}$ ligand takes μ_4 coordination mode linking Mn2B, Mn2C, Mn2F and Mn1 using the *syn,syn* carboxylate and the μ_2 oxygen atoms of N-oxide group. The detailed bond lengths and angles are summarized in Table 2. In that way, one Mn1 ions and two crystallographically equivalent Mn2 ions were bridged by the carboxylate/N-oxide groups forming a trimer, then the adjacent trimers were linked by double carboxylate to give a carboxylate/N-oxide mixed bridged 1D chain. In the chain the adjacent Mn…Mn distances of Mn1…Mn2 and Mn2…Mn2 are 3.919 and

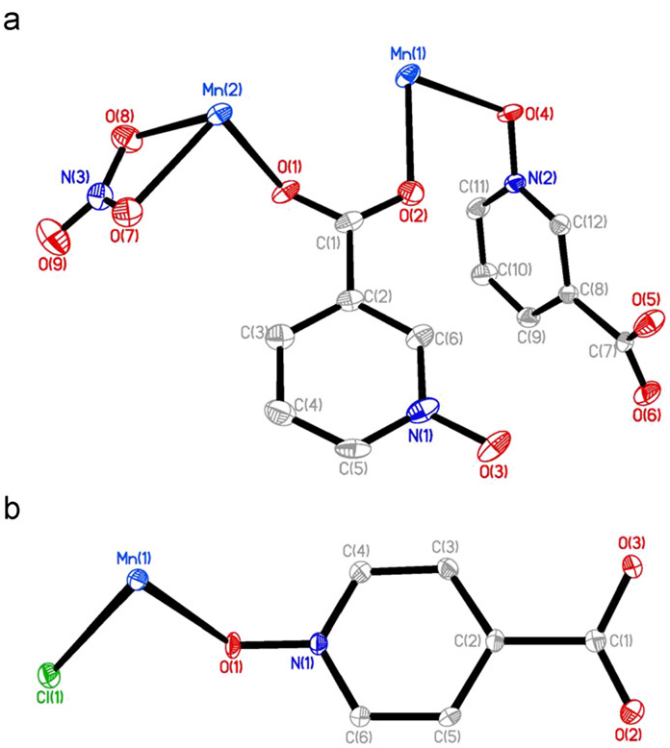

Fig. 1. The asymmetric crystallographic units of the complexes showing displacement ellipsoids at the 30% probability level. H atoms have been omitted: (a) for **1** and (b) for **2**.

4.686 Å, respectively. The 2D structure of **1** can be described as a carboxylate/N-oxide mixed bridged chain joined by the nicotinate ligands (Fig. 3). In topological, Mn1 ions can be described as 6-connecting nodes and Mn2 ions can be described as 4-connecting nodes; meanwhile the two types of nicotinate N-oxide ligands can be described as 3-connecting nodes and 4-connecting nodes, respectively. Thus 2D net can be viewed as a 3, 4, 6-connected 4-nodal net with Schläfli notation [4.4.4.4.6(2).6(2)][4.4.4][4.4.4.4.4.4.6.6.6(2).6(2).6(2).6(2).8(4).8(4).8(8)][4.4.4.4.6(2).6(3)] ({4^3}2{4^4; 6^2}4{4^6; 6^6; 8^3}) (Fig. 4a). To the best of our knowledge, such a net is unprecedented yet [14].

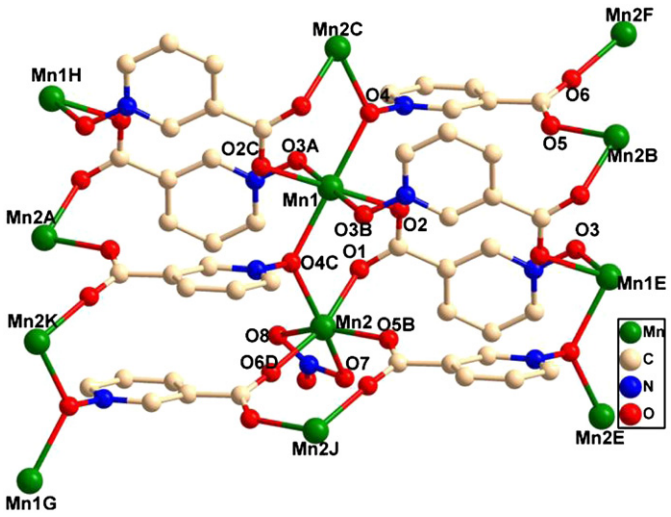

Fig. 2. View of the coordination environment of Mn^{II} ions and linkage of the ligands in **1**.

[Mn$\mathbf{L^2}$Cl]$_n$ (**2**). Complex **2** crystallized in the space group *Pbca* and the asymmetric unit of **2** has a Mn^{II} ion, one $\mathbf{L^2}$ ligand and one chlorine anion (Fig. 1b). Mn1 ions are in octahedral coordinated environment (MnO_4Cl_2) with Mn–O=2.0–2.3 Å and Mn–Cl=2.5–2.7 Å (Fig. 5). The chlorine anion in μ_2 mode bridges Mn1 and Mn1D with a Mn1–Cl1–Mn1D angle 94.28(3)°. The $\mathbf{L^2}$ anions coordinated to Mn1, Mn1D, Mn1E and Mn1F with the *syn,syn* carboxylate and μ_2 mode N-oxide group (Fig. 5). As shown in Fig. 6, the structure of **2** can be comprehended as that, first a N-oxide/Cl mixed coordinated Mn^{II} chain was formed, then double *syn,syn* carboxylate linked the neighbor chains forming a honeycomb layer, finally the layers are connected by the pyridine ring of the $\mathbf{L^2}$ to give a 3D framework. The distances of the neighbor layers are about 8.3 Å (Fig. 7). Topologically, the $\mathbf{L^2}$ coordinating four Mn^{II} ions can be described as a 4-connected node, while the Mn^{II} ions linked by four $\mathbf{L^2}$ and two other Mn^{II} ions though the chlorine could be defined as a 6-connected node. Thus a 4, 6-connected binodal net Schläfli notation [3.4.5.5.5.5][3.3.4.5.5.5.5.5.5.6.6.6.6.6.6] ({3;4;5^4} {3^2;4;5^6;6^6}) net can be deduced from **2** (Fig. 4b). The honeycomb layer

Table 2
Selected bond lengths [Å] and angles for complexes **1** and **2** [deg].

1			
Mn(1)–O(3)#1	2.121(5)	Mn(2)–O(6)#4	2.089(4)
Mn(1)–O(3)#2	2.121(5)	Mn(2)–O(5)#2	2.109(4)
Mn(1)–O(2)	2.213(4)	Mn(2)–O(1)	2.138(4)
Mn(1)–O(2)#3	2.213(4)	Mn(2)–O(4)#3	2.186(4)
Mn(1)–O(4)#3	2.293(4)	Mn(2)–O(7)	2.260(4)
Mn(1)–O(4)	2.293(4)	Mn(2)–O(8)	2.334(5)
Mn(2)#3–O(4)–Mn(1)	122.10(16)		
#1 $x-1, y, z$	#2 $-x+2, -y+1, -z$	#3 $-x+1,-y+1,-z$	#4 $x-1,y,z-1$
2			
Mn(1)–O(2)#1	2.093(3)	Mn(1)–Cl(1)#3	2.5207(12)
Mn(1)–O(3)#2	2.154(3)	Mn(1)–Cl(1)	2.6020(11)
Mn(1)–O(1)#3	2.225(3)	Mn(1)–O(1)	2.244(3)
Mn(1)#4–Cl(1)–Mn(1)	94.28(3)	Mn(1)#4–O(1)–Mn(1)	114.35(10)
#1 $x,-y+1/2,z+1/2$	#2 $-x,y+1/2,-z+3/2$	#3 $-x+1/2,y+1/2,z$	#4 $-x+1/2,y-1/2,z$

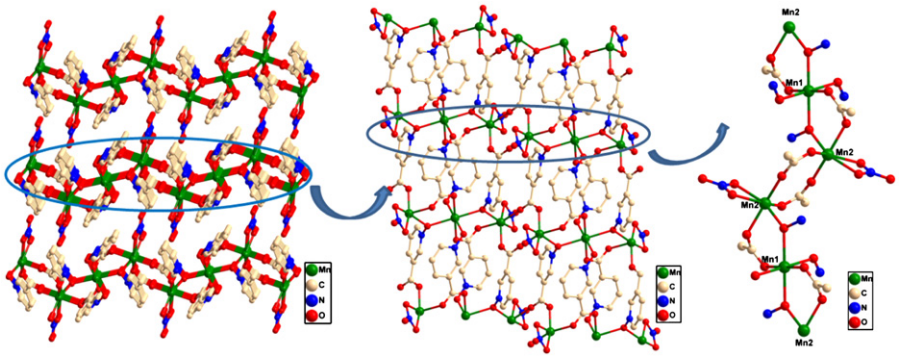

Fig. 3. View of the 3D packing, 2D layer and the 1D chain structure of **1**.

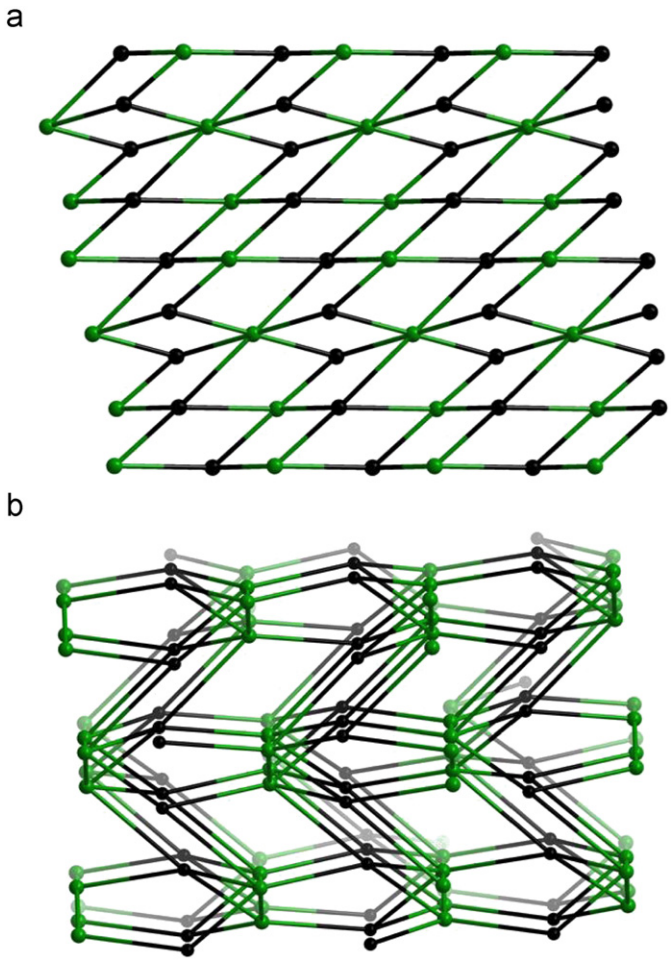

Fig. 4. (a) View of the 2D network topology of **1**. (b) View of the 3D network topology of **2**. Mn^{II} ions was in green and $\mathbf{L^1/L^2}$ in black.

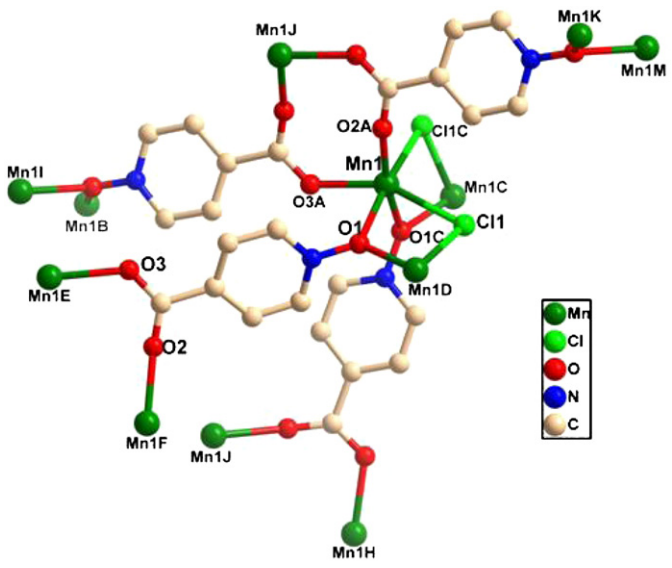

Fig. 5. View of the coordination environment of Mn^{II} ions and linkage of the ligands in **2**.

structure of **2** was similar to that reported by Wang et al. [8a], but the linkage of $\mathbf{L^2}$ between the layers does not have the same result in different topology.

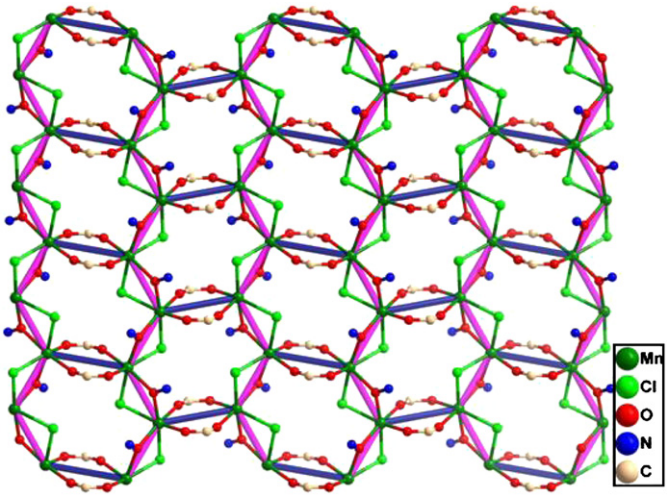

Fig. 6. The 2D layer structure honeycomb of **2**.

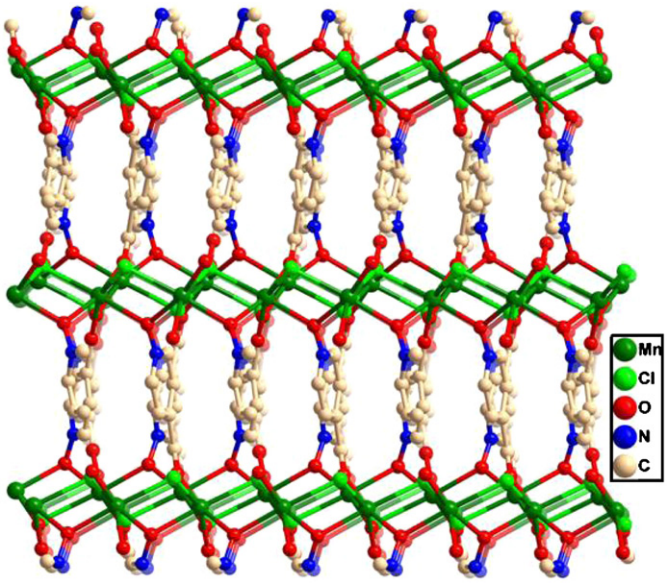

Fig. 7. View of the 3D structure of **2**.

It is worth noting that the little anions such as nitrate anion and chlorine anions in **1** and **2** are significant in forming those complexes, in which the pyridine carboxylate N-oxide ligand coordinated to four divalence metal ions in octahedron geometry. If the $\mathbf{L^1/L^2}$ ligand coordinated to three divalence octahedral metal ions the positive and negative charges are just equivalent. While here $\mathbf{L^1/L^2}$ take μ_4 modes coordinating four divalence metal ions, additional anions with less coordinated number are needed. That situation was also found in a similar work reported by Yan et al. [9a]. In Yan's work the azide anions acting as the additional anions lead to the $\mathbf{L^2}$ in μ_4 modes or $\mathbf{L^1/L^2}$ in μ_3 modes but one water molecule coordinate to the metal ions. When azide anions were co-ligands, unique azide/carboxylate mixed coordinated chains were formed. However, in this work alternating chain or honeycomb layer structures were found. In order to investigate the effect of the anions, we try the reaction of $\mathbf{L^1/L^2}$ with other salt but no suitable crystal for X-ray diffraction was obtained.

3.2. Magnetic properties

Magnetic measurements were carried out on crystalline samples of complexes **1** and **2,** which were pure-phase (confirmed

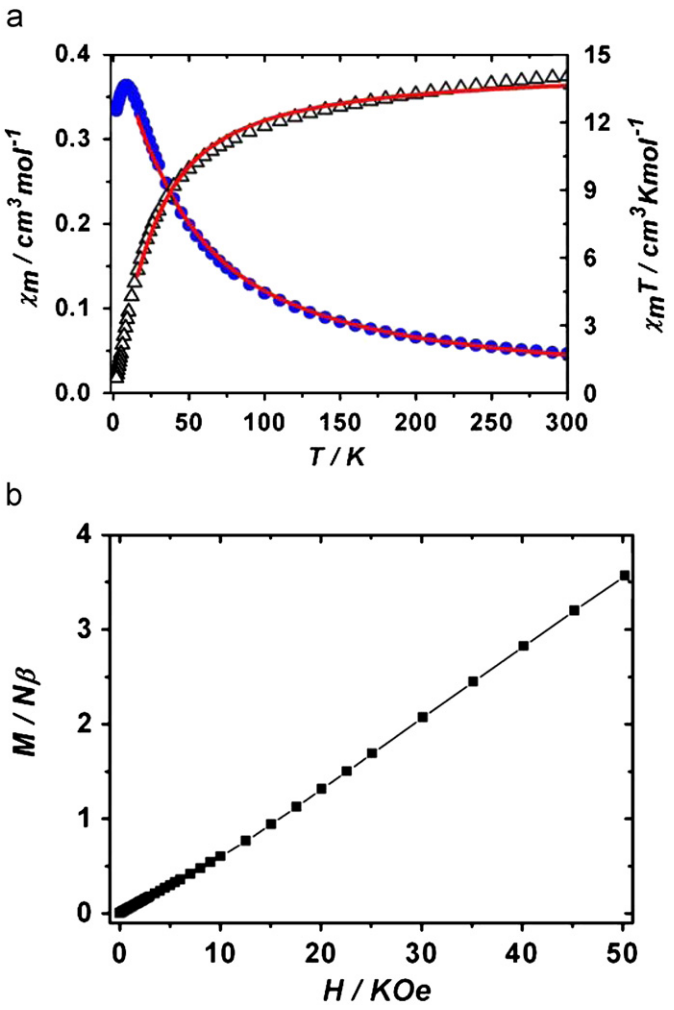

Fig. 8. (a) χ_m vs. T (circles) and $\chi_m T$ vs. T (triangle) plots of **1**. The solid line is the best fit to the experimental data. (b) Magnetization vs. field plot at 2.0 K for **1**.

by XRPD, see Fig. S1). The magnetic susceptibilities of **1** collected in the 2–300 K temperature range under 1 kOe are shown as Fig. 8a. The $\chi_m T$ value (14.02 $cm^3\,K\,mol^{-1}$) at 300 K agrees with the spin-only value of three octahedral Mn^{II} ions. As the temperature decreases, the χ_m product increases and gives a peak at 9 K and then decreases, while the $\chi_m T$ product decreases continually down to a minimum value of 0.67 $cm^3\,K\,mol^{-1}$ at 2 K. Fitting the data at 25–300 K with the Curie–Weiss law gives $C=15.1\ cm^3\,mol^{-1}\,K$ and $\theta=-27.4$ K (Fig. S2a). The negative value of θ and the initial decrease of $\chi_m T$ should be due to the overall antiferromagnetic coupling between the Mn^{II} ions. Based on the structure the magnetic behavior mainly depended the 1D Mn^{II} chain with $-J_1J_1J_2-$ magnetic coupling Mn^{II} sequence. In that chain J_1 coupling is the interaction between Mn1 and Mn2 conducted by the mixed N-oxide and *syn,syn* carboxylate bridges. The interaction transferred by the double *syn,syn* carboxylate between two Mn2 is J_2. To evaluate the interactions, with the molecular field approximation, a least-squares fit of the observed magnetic data based on the theoretical expression of 1D Heisenberg chains with alternating interactions $-J_1J_1J_2-$, proposed by Escuer et al. [15], was made. The model provides a proper fit of $\chi_m T$ variation over the temperature range 16–300 K, giving the best parameters $J_1=-2.77\ cm^{-1}$, $J_2=-0.67\ cm^{-1}$, $zj'=-0.0002\ cm^{-1}$, $g=2.10$. $R=3.62\times10^{-4}$ $(R=\sum[(\chi_m T)_{obs}-(\chi_m T)_{calc}]^2/[(\chi_m T)_{obs}]^2)$, which agree with the structure character pretty well. Usually, the *syn,syn* carboxylate between Mn^{II} ions transfer antiferromagnetic interaction with several exceptions [16,17]. The N-oxide would also conduct antiferromagnetic coupling for the larger Mn–O–Mn angle 122° [18]. The small magnitude of the J_2 may be due to the long Mn…Mn distances. The peak of the χ_m vs T curve at 9 K indicated **1** was an antiferromagnet and T_N was determined from the peak of the $d(\chi_m T)/dT$ at 6.3 K. The magnetic properties of **1** show low-dimensional characteristic for the ratio of $T_N/T(\chi_{max})$ of 0.7 is significantly lower than that for a 3D antiferromagnet [19], which agrees with the structure character of complex **1**. The magnetization is 3.6 $N\beta$ for **1** at 50 kOe, far from the saturation value of the three Mn^{II} ions (15 $N\beta$ for $g=2$), suggesting again the antiferromagnet ordering (Fig. 8b).

The temperature dependence of the magnetic susceptibility of **2** collected under 2000 Oe in 2–300 K is shown in Fig. 9a. The $\chi_m T$ value (4.17 $cm^3\,K\,mol^{-1}$) at 300 K agrees with the spin-only value of one octahedral Mn^{II} ion. As the temperature decreases, the χ_m product increases and gives a peak at 7 K and then decreases, while the $\chi_m T$ product decreases continually down to a minimum value of 0.31 $cm^3\,K\,mol^{-1}$ at 2 K. Fitting the data at 40–300 K with the Curie–Weiss law gives $C=4.37\ cm^3\,mol^{-1}\,K$ and $\theta=-10.48$ K (Fig. S2b). Based on the structure the magnetic behavior was mainly in the person of the character of the 2D honeycomb Mn^{II} layer with two different coupling constants J_1 and J_2, in which J_1 is the interaction though the N-oxide/Cl bridges and J_2 for that of double *syn,syn* carboxylate (Fig. 6). The data of the magnetic susceptibility in 16–300 K were fitted by the

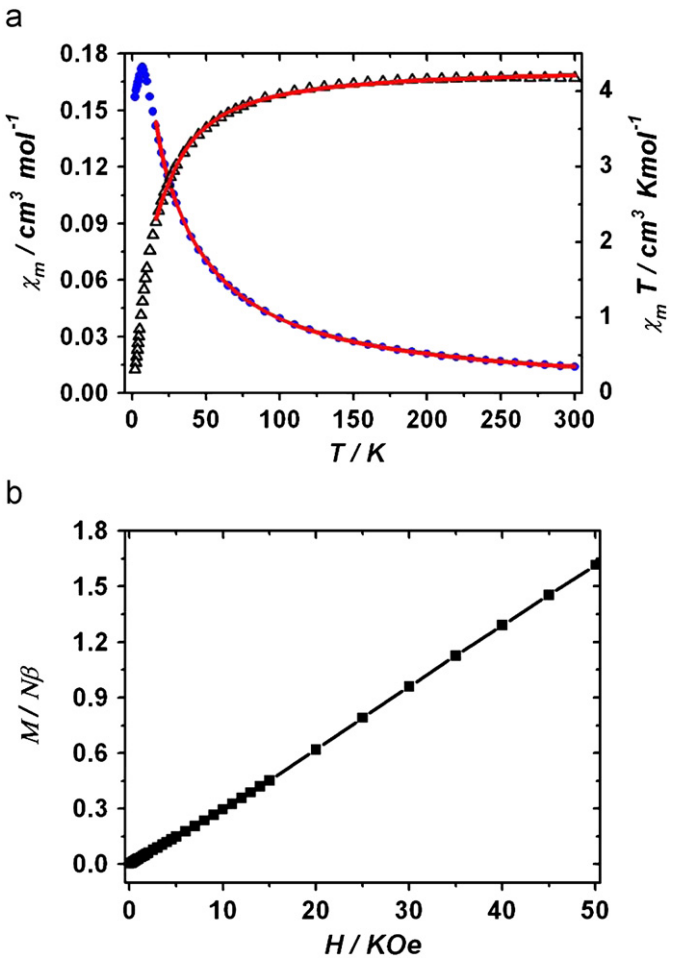

Fig. 9. (a) χ_m vs. T (circles) and $\chi_m T$ vs. T (triangle) plots of **2**. The solid line is the best fit to the experimental data. (b) Magnetization vs. field plot at 2.0 K for **2**.

Curély's [20] model (see the Supporting Information), giving the best fit with parameters $J_1 = -2.05\ cm^{-1}$, $J_2 = 0.55\ cm^{-1}$, $g = 1.99$, $R = 1.80 \times 10^{-5}$ $(R = \sum[(\chi_m T)_{obs} - (\chi_m T)_{calc}]^2/[(\chi_m T)_{obs}]^2)$. The N-oxide and Cl bridges between Mn^{II} ions would conduct antiferromagnetic coupling for the Mn–O–Mn and Mn–Cl–Mn angles of 114° and 94°, respectivly [18]. However, the weak ferromagnetic coupling of $0.55\ cm^{-1}$ mediated by the double *syn,syn* carboxylate is uncommon. As mentioned above, there are only a few examples that the *syn,syn* carboxylate transferred weak ferromagnetic coupling between Mn^{II} ions [17]. In this case the carboxylate and the Mn^{II} ions are not in an-plane strictly, which may lead to distinct magnetic orbitals overlap with weak ferromagnetic interactions. The peak of the χ_m vs T curve at 6 K indicated **2** was an antiferromagnet and the T_N was determined from the peak of the $d(\chi_m T)/dT$ at 6.2 K. The magnetization is 1.65 $N\beta$ for **2** at 50 kOe, far from the saturation value of the three Mn^{II} ions (5 $N\beta$ for $g=2$), suggesting again the antiferromagnet ordering (Fig. 9b).

4. Conclusion

Two new coordination compounds with pyridine carboxylate N-oxide ligands were synthesized and structurally characterized. The N-oxide groups enrich the coordinated mode of the ligands, while the other negative charge ligands are significant for the charge balance in the complexes in which the pyridine carboxylate N-oxide ligands take μ_4 bridging mode. Magnetic study indicated that weak antiferromagnetic coupling was conducted by the N-oxide group between Mn^{II} ions. The magnetic behaviors of **1** and **2** reflected the structure character of the 1D alternating chains and 2D honeycomb layers, respectively.

Acknowledgement

This work was supported by the National Natural Science Foundation of China (Nos. 20801041 and 20771082).

Appendix A. Supplementary materials

Supplementary data associated with this article can be found in the online version at doi:10.1016/j.jssc.2010.06.010.

References

[1] (a) B. Moulton, M.J. Zaworotko, Chem. Rev. 101 (2001) 1629–1658 For example:;
(b) M. Eddaoudi, D.B. Moler, H. Li, B. Chen, T.M. Reineke, M. O'Keeffe, O.M. Yaghi, Acc. Chem. Res. 34 (2001) 319–330;
(c) X. Zhao, B. Xiao, A.J. Fletcher, K.M. Thomas, J. Am. Chem. Soc. 109 (2005) 8880–8888;
(d) E.J. Schelter, A.V. Prosvirin, K.R. Dunbar, J. Am. Chem. Soc. 126 (2004) 15004–15005.
[2] (a) W.-P. Su, M.-C. Hong, J.-B. Weng, R. Cao, S.-F. Lu, Angew. Chem. Int. Ed. 39 (2000) 2911–2914 For example:;
(b) W. Chen, H.-M. Yuan, J.-Y. Wang, Z.-Y. Liu, J.-J. Xu, M. Yang, J.-S. Chen, J. Am. Chem. Soc. 125 (2003) 9266–9267;
(c) M.-L. Tong, X.-M. Chen, S.R. Batten, J. Am. Chem. Soc. 125 (2003) 16170–16171;
(d) W.-S. Liu, T.-Q. Jiao, Y.-Z. Li, Q.-Z. Liu, H.-W.ang M.-Y. Tan, L.-F. Wang, J. Am. Chem. Soc. 126 (2004) 2280–2281.
[3] (a) X.-H. Bu, M.-L. Tong, H.-C. Chang, S. Kitagawa, S.R. Batten, Angew. Chem. Int. Ed. 43 (2004) 192–195 For example:;
(b) X.-Y. Wang, L. Wang, Z.-M. Wang, S. Gao, J. Am. Chem. Soc. 128 (2006) 674–675;
(c) J.-P. Zhao, B.-W. Hu, Q. Yang, T.-L. Hu, X.-H. Bu, Inorg. Chem. 48 (2009) 7111–7116;
(d) E. Cariati, X. Bu, P.C. Ford, Chem. Mater. 12 (2000) 3385–3391.
[4] (a) Y.-B. Dong, H.-Y. Wang, J.-P. Ma, D.-Z. Shen, R.-Q. Huang, Inorg. Chem. 44 (2005) 4679–4692 For example:;
(b) J.-R. Li, Y. Tao, Q. Yu, X.-H. Bu, Chem. Commun. (2007) 1527–1529;
(c) N. Snejko, C. Cascales, B. Gomez-Lor, E. Gutiérrez-Puebla, M. Iglesias, C. Ruiz-Valero, M.A. Monge, Chem. Commun. (2002) 1366–1367.
[5] (a) J.S. Hall, J.G. Loeb, K.H. Shimizu, G.P.A. Yap, Angew. Chem. Int. Ed. 37 (1998)121-123 37 (1998);
(b) R.D. Schnebeck, E. Freisinger, B. Lippert, Angew. Chem. Int. Ed. 38 (1999) 168–171.
[6] (a) J.-R. Li, R.-H. Zhang, X.-H. Bu, Cryst. Growth Des. 4 (2004) 219–221;
(b) X.-L. Tong, D.-Z. Wang, T.-L. Hu, W.-C. Song, Y. Tao, X.-H. Bu, Cryst. Growth Des. 9 (2009) 2280–2286;
(c) D.B. Cordes, A.S. Bailey, P.L. Caradoc-Davies, D.H. Gregory, L.R. Hanton, K. Lee, M.D. Spicer, Inorg. Chem. 44 (2005) 2544–2552;
(d) J.-X. Meng, Y. Lu, Y.-G. Li, H. Fu, E.-B. Wang, Cryst. Growth Des. 9 (2009) 4116–4126.
[7] (a) P.C.M. Duncan, D.M.L. Goodgame, S. Menzer, D.J. Williams, Chem. Commun. (1996) 2127–2128;
(b) L. Carlucci, G. Ciani, D.W. Gudenberg, D.W. Proserpio, Inorg. Chem. 36 (1997) 3812–3813;
(c) X.-H. Bu, W. Chen, W.-F. Hou, M. Du, R.-H. Zhang, F. Brisse, Inorg. Chem. 41 (2002) 3477–3482;
(d) G.-H. Cui, J.-R. Li, J.-L. Tian, X.-H. Bu, S.R. Batten, Cryst. Growth Des. 5 (2005) 1775–1780;
(e) J.-R. Li, M. Du, X.-H. Bu, R.-H. Zhang., J. Solid State Chem. 173 (2003) 20–26.
[8] (a) Y.-H. Zhao, H.-B. Xu, Y.-M. Fu, K.-Z. Shao, S.-Y. Yang, Z.-M. Su, X.-R. Hao, D.-X. Zhu, E.-B. Wang, Cryst. Growth Des. 8 (2008) 3566–3576;
(b) J.-H. Jian, A.J. Blake, N.R. Champness, P. Hubberstey, C. Wilson, M. Schroder, Inorg. Chem. 47 (2008) 8652–8664.
[9] (a) Z. He, Z.-M. Wang, S. Gao, C.-H. Yan, Inorg. Chem. 45 (2006) 6694–6705;
(b) B.-P. Yang, H.-Y. Zeng, Z.-C. Dong, J.-G. Mao, J. Coord. Chem. 56 (2003) 1513–1523.
[10] (a) Y.-H. Zhao, H.-B. Xu, K.-Z. Shao, Y. Xing, Z.-M. Su, J.-F. Ma, Cryst. Growth Des. 7 (2007) 513–520;
(b) Z. He, Z.-M. Wang, C.-H. Yan, Cryst. Eng. Commun. 7 (2005) 143–150.
[11] B.-W. Sun, S. Gao, B.-Q. Ma, D.-Z. Niu, Z.-M. Wang, J. Chem. Soc. Dalton Trans. (2000) 4187–4191.
[12] A.X.S. Bruker, in: SAINT Software Reference Manual, Madison, WI, 1998.
[13] (a) G.M. Sheldrick, SADABS, Siemens Area Detector Absorption Corrected Software, University of Göttingen, Germany, 1996;
(b) G.M. Sheldrick, SHELXTL NT Version 5.1. Program for Solution and Refinement of Crystal Structures, University of Göttingen, Germany, 1997.
[14] Reticular Chemistry Structure Resource (RCSR), 〈http://rcsr.anu.edu.au/〉; Euclidean Patterns in Non-Euclidean Tilings (EPINET), 〈http://epinet.anu.edu.au/〉;
V.A. Blatov, A.P. Shevchenko, TOPOS 4.0, Samara State University, Russia.
[15] (a) M.A.M. Abu-Youssef, M. Drillon, A. Escuer, M.A.S. Goher, F.A. Mautner, R. Vicente, Inorg. Chem. 39 (2000) 5022–5027;
(b) M.-H. Zeng, M.-C. Wu, H. Liang, Y.-L. Zhou, X.-M. Chen, S.W. Ng, Inorg. Chem. 46 (2007) 7241–7243.
[16] (a) G. Fernández, M. Corbella, J. Mahía, M.A. Maestro, Eur. J. Inorg. Chem. (2002) 2502–2510;
(b) B. Albela, M. Corbella, J. Ribas, I. Castro, J.H. Sletten, Stoeckli-Evans, Inorg. Chem. 37 (1998) 788–789;
(c) P.S. Mukherjee, S. Konar, E. Zangrando, T. Mallah, J. Ribas, N.R. Chaudhuri, Inorg. Chem 42 (2003) 2695–2730 and references therein.
[17] (a) X.-S. Tan, J. Sun, D. Feng, D.-F. Xiang, W.-X. Tang, Inorg. Chim. Acta 255 (1997) 157–161;
(b) D. Mandal, P.B. Chatterjee, S. Bhattacharya, K.-Y. Choi, R. Clérac, M. Chaudhury, Inorg. Chem. 48 (2009) 1826–1835.
[18] (a) J.B. Goodenough, Magnetism and the Chemical Bond, NewYork, Wiley, 1963;
(b) Z.-M. Wang, B. Zhang, H. Fujiwara, H. Kobayashi, M. Kurmooc, Chem. Commun. (2004) 416–417;
(c) J.-P. Zhao, B.-W. Hu, Q. Yang, X.-F. Zhang, T.-L. Hu, X.-H. Bu, Dalton Trans. 1 (2010) 56–58.
[19] G.C. DeFotis, E.D. Remy, C.W. Scherrer, Phys. Rev. B: Condens. Matter Mater. Phys. 41 (1990) 9074–9086.
[20] J. Curély, F. Lloret, M. Julve, Phys. Rev. B 58 (1998) 11465–11483.